0026-895X/00/030649-00$3.00/0
MOLECULAR PHARMACOLOGY
Vol. 58, No. 3
13175/848108
*Mol Pharmacol* 58:649–658, 2000
*Printed in U.S.A.*


# Acridinecarboxamide Topoisomerase Poisons: Structural and Kinetic Studies of the DNA Complexes of 5-Substituted 9-Amino-(*N*-(2-dimethylamino)ethyl)acridine-4-Carboxamides

ADRIENNE ADAMS, J. MITCHELL GUSS, CHARLES A. COLLYER, WILLIAM A. DENNY, ARUNGUNDRUM S. PRAKASH, and LAURENCE P. G. WAKELIN

*Department of Biochemistry, University of Sydney, New South Wales, Australia (A.A., J.M.G., C.A.C.); Auckland Cancer Society Research Centre, Faculty of Medicine and Health Science, University of Auckland, Auckland, New Zealand (W.A.D.); National Centre for Environmental Toxicology, Coopers Plains, Queensland, Australia (A.S.P.); and School of Physiology and Pharmacology, University of New South Wales, New South Wales, Australia (L.P.G.W.)*

Received December 16, 1999; accepted June 12, 2000

This paper is available online at http://www.molpharm.org

## ABSTRACT

For a series of antitumor-active 5-substituted 9-aminoacridine-4-carboxamide topoisomerase II poisons, we have used X-ray crystallography and stopped-flow spectrophotometry to explore relationships between DNA binding kinetics, biological activity, and the structures of their DNA complexes. The structure of 5-F-9-amino-[*N*-(2-dimethylamino)ethyl]-acridine-4-carboxamide bound to $d(CGTACG)_2$ has been solved to a resolution of 1.55 Å in space group $P6_4$. A drug molecule intercalates between each of the CpG dinucleotide steps, its protonated dimethylamino group partially occupying positions close to the N7 and O6 atoms of guanine G2 in the major groove. A water molecule forms bridging hydrogen bonds between the 4-carboxamide NH and the phosphate group of the same guanine. Intercalation unwinds steps 1 and 2 by 12° and 8°, respectively compared with B-DNA, whereas the central TpA step is overwound by 10°. Nonphenyl 5-substituents, on average, decrease mean DNA dissociation rates by a factor of three, regardless of their steric, hydrophobic, H-bonding, or electronic properties. Cytotoxicity is enhanced on average 4-fold and binding affinities rise by 3-fold, thus there is an apparent association between kinetics, affinity, and cytotoxicity. Taken together, the structural and kinetic studies imply that the main origin of this association is enhanced stacking interactions between the 5-substituent and cytosine in the CpG binding site. Ligand-dependent perturbations in base pair twist angles and their consequent effects on base pair-base pair stacking interactions may also contribute to the stability of the intercalated complex. 5-Phenyl substituents modify dissociation rates without affecting affinities, and variations in their biological activity are not correlated with DNA binding properties, which suggests that they interact directly with the topoisomerase protein.

DNA intercalating agents that form ternary complexes with topoisomerase II, trapping the enzyme in the "cleavable complex" stage of its catalytic cycle, are prominent in the treatment of cancer (Denny, 1997; Malonne and Atassi, 1997). Notable examples include the anthracycline antibiotics doxorubicin and daunomycin, the anthracenedione mitoxantrone, and the 9-anilinoacridine amsacrine (Malonne and Atassi, 1997). Work by Denny and colleagues with intercalating acridinecarboxamide derivatives established that 9-aminoacridine-4-carboxamides are also potent topoisomerase II-poisoning cytotoxins with activity against mouse leukemia models in vivo (Atwell et al., 1984; Denny et al., 1986; Finlay et al., 1996). Studies of acridine substitution patterns among the 9-aminoacridine-4-carboxamides revealed that substituents in the 5-position either enhance cytotoxic and antileukemic potency or, when strongly electron withdrawing, promote solid tumor activity (Rewcastle et al., 1986; Denny et al., 1987). The related des-9-amino compound, *N*-[2-(dimethylamino)ethyl]acridine-4-carboxamide (DACA; NSC 601316), which inhibits both topoisomerase I and II (Schneider et al., 1988; Finlay et al., 1996), has a wide spectrum of activity against solid tumors in animal models and is currently in clinical trial (Atwell et al., 1987; Baguley et al., 1995; Kestell et al., 1999; McCrystal et al., 1999).

The parent compound 9-amino-DACA (Fig. 1) is a dication at neutral pH ($pK_a$ values of 8.3 and 10) that intercalates into DNA with an unwinding angle of 17° (Palmer et al., 1988), has an affinity of $4 \times 10^5\ M^{-1}$ for calf thymus DNA in 100 mM NaCl at pH 7.0 (Crenshaw et al., 1995), and binds preferentially to GC-rich nucleotide sequences (Bailly et al., 1992). There are tight correlations between ligand structure, cytotoxicity, and DNA binding kinetics for the 9-aminoacridine-4-carboxamide

This work was supported by grants from the Association for International Cancer Research (to L.P.G.W., C.A.C., A.A.) and the University of Sydney Faculty of Medicine (to A.A., J.M.G., L.P.G.W.).

**ABBREVIATIONS:** DACA, *N*-[2-(dimethylamino)ethyl]acridine-4-carboxamide; MPD, 2-methyl-2,4-pentanediol; F, fluoro.

class of compounds (Atwell et al., 1984; Denny et al., 1986, 1987; Rewcastle et al., 1986; Wakelin et al., 1987). The most significant features of the structure activity relationships are that the side chain must be in the acridine 4 position, the carboxamide must have an unsubstituted NH group, and that there must be two methylene groups between the carboxamide NH and the terminal protonated *N*,*N*-dimethylamino group (Atwell et al., 1984). These findings, coupled with the dependence of the dissociation kinetics profile on ligand structure (Wakelin et al., 1987), imply that the side chain makes specific interactions with the DNA that are sensed by topoisomerase II in the ternary complex. To provide insight into the nature of these molecular interactions, we have recently presented crystal structures of 9-amino-DACA bound to the DNA hexanucleotide $d(CGTACG)_2$ (Adams et al., 1999) and of 6-bromo-9-amino-DACA bound to the brominated hexanucleotide $d(CG^{5Br}UACG)_2$ (Todd et al., 1999), where the ligand is intercalated at the CpG dinucleotide steps. In both complexes, the carboxamide group forms an internal hydrogen bond with the protonated N10 atom of the acridine ring and the side chain lies in the DNA major groove with its protonated *N*,*N*-dimethylamino group forming hydrogen-bonding interactions with the O6 and N7 atoms of guanine G2. In each case, a hydrogen-bonded water molecule bridges the NH of the carboxamide group to the guanine G2 phosphate at the intercalation site. These structures have provided a molecular rationale for understanding the structure activity relationships for antitumor activity and enabled a mechanistic interpretation of the dependence of kinetics on ligand structure (Adams et al., 1999). In particular, they have permitted the critical step in the dissociation kinetics profile that correlates with cytotoxicity and antitumor activity to be identified with the side chain-guanine interaction (Wakelin et al., 1987; Adams et al., 1999).

In this study, we have investigated the dissociation kinetics of DNA complexes of 5-substituted derivatives of 9-amino-DACA to probe correlations between ligand structure, kinetic profiles, DNA-ligand residence times, and biological activity. In addition, we have determined the crystal structure of one of their number, 5-F-9-amino-DACA (Fig. 1), bound to $d(CGTACG)_2$. Our objective is to gain an understanding of the features of the DNA-ligand interaction that promote antitumor efficacy and control the spectrum of antitumor activity among the acridine-4-carboxamides. The 5-substituents are either aliphatic or aromatic and vary with respect to size, lipophilicity, and electron withdrawing/donating abilities. We have interpreted our kinetic results in terms of the crystal structures and for the nonphenyl substituents find a general relationship between DNA residence time, DNA affinity, and cytotoxic potency. The principal origin of this association seems to be increased stacking interactions between the 5-substituent and cytosine in the CpG intercalation site. 5-Phenyl substituents modify dissociation rates without affecting affinities, and variations in their biological activity are not correlated with DNA binding properties, which suggests that they interact directly with the topoisomerase protein.

## Experimental Procedures

**Materials.** All 9-aminoacridine-4-carboxamides were synthesized as their hydrochloride salts and purified in the Auckland Cancer Society Research Center as previously described (Denny et al., 1987). The purified self-complementary deoxyribonucleotide CGTACG was purchased from Oswel Research Products Ltd (University of Southampton, UK). Calf thymus DNA was purchased from the Sigma Chemical Company (St. Louis, MO).

**Crystallization and Diffraction Data Collection.** The lyophilized hexanucleotide was dissolved in water to give a 2.4 mM stock solution which was stored frozen at 253 K. 5-F-9-amino-DACA (Fig. 1) was dissolved in water to give a 10 mM stock solution which was also stored frozen at 253 K. Crystals were grown at 291 K by vapor diffusion in sitting drops using the Hampton Nucleic Acid Mini Screen (Hampton Research, El Lazo Road, CA). Yellow bullet-shaped crystals (approximate dimensions, 0.25 × 0.20 × 0.20) grew in 3 months from drop 16 of the screen which contained 3.3% 2-methyl-2,4-pentanediol (MPD), 13.3 mM sodium cacodylate buffer, pH 7.0, 4 mM spermine tetrahydrochloride, 26.7 mM NaCl, 6.7 mM $MgCl_2$, 0.8 mM DNA (double-stranded), and 1.6 mM 5-F-9-amino-DACA equilibrated against 35% MPD. A crystal was removed from the drop, placed in Riedel de Haen perfluoropolyether RS 3000 oil, mounted in a cryoloop, and frozen at 110 K in a $N_2$ cryostream. Diffraction intensities were recorded on a Rigaku R-axis II image plate system mounted on a Rigaku RU-200 rotating anode generator with focusing mirror optics (CuK$\alpha$, 1.5418 Å). Data were collected in two passes at a crystal-to-detector distance of 65 mm; the second pass was at a shorter exposure time of 10 min, compared with 25 min, and at reduced power to allow base pair-stacking reflections with d ≈ 3.4 Å to be recorded accurately without overloading the image plate. The data were processed to 1.55 Å resolution with the DENZO and SCALEPACK program (Otwinowski, 1993) which indicated this crystal form to be in the space group $P6_4$ (or $P6_2$) with a = 30.1 Å and c = 39.4 Å (Table 1). Every 12th reflection was separated into a reference set to monitor $R_{free}$.

**Structure Solution and Refinement.** The hexagonal crystal form reported here is isomorphous to crystals of $d(CGTACG)_2$ complexed with 9-amino-DACA (Adams et al., 1999; Nucleic Acid Databank accession number DD0015). This complex was refined in space group $P6_4$ (a = 30.2 Å, c = 39.7 Å) at 1.6 Å resolution with an asymmetric unit composed of a single strand of DNA, an intercalated drug molecule, and an end-stacked drug molecule. The elements of this structure chosen as a starting model for refinement were one strand of $d(CGTACG)_2$ and

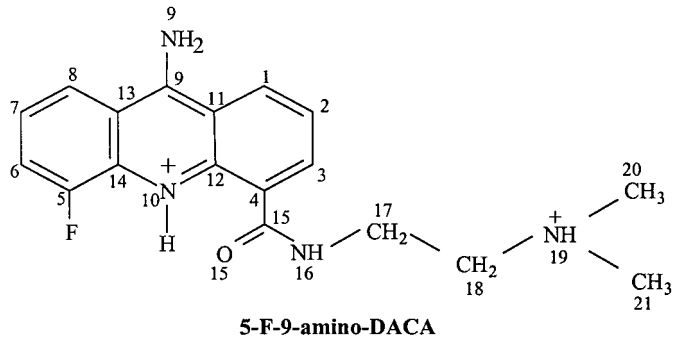


**5-F-9-amino-DACA**

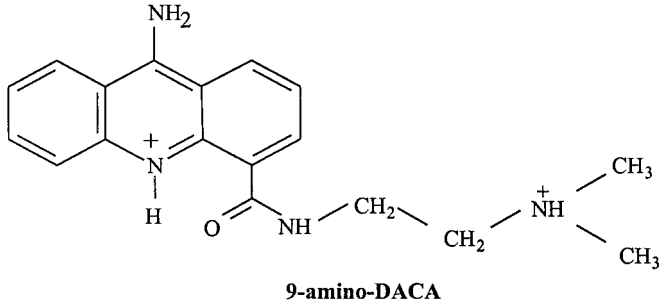


**9-amino-DACA**

**Fig. 1.** Structures of 5-F-9-amino-DACA and 9-amino-DACA.

the chromophore of the intercalated and end-stacked drug molecules. The initial temperature factors were those of the starting structure; the initial R factor was 31.4% and $R_{free}$ was 36.2% for data in the resolution shell 16 to 1.55 Å. An iterative refinement procedure was conducted using the program SHELXL-97 (Sheldrick, 1997) interspersed with inspection of electron density maps and manual model rebuilding with the program O (Jones et al., 1991). Bond lengths and bond angles within the DNA bases were restrained to target values as specified by Taylor and Kennard (1982). All other chemically equivalent DNA bond lengths and bond angles were restrained by similarity distance restraints but without specification of an actual target value. For 5-F-9-amino-DACA, bond lengths and bond angles were restrained to specified target values generated from an idealized structure built with INSIGHT II and optimized with an AMBER force field using the DISCOVER program (INSIGHT II User Guide, 1995). The DNA bases, the acridine ring, and the carboxamide group of 5-F-9-amino-DACA were restrained to be planar, whereas all other torsion angles remained unrestrained.

As the refinement proceeded, electron density corresponding to positions of atoms not included in the model was observed. The positions of the 5-fluorines could be clearly seen and were included in the model. At points where the density was unequivocal, water molecules were included. Regions of diffuse solvent were modeled using Babinet's principle as implemented in the SWAT command in SHELXL-97 (Sheldrick, 1997). The side chains of the drugs were introduced into the refinement one at a time. For both intercalated and end-stacked drugs, the positions of the carboxamide group and the C17 carbon atoms were clear on the difference density maps. Density for the remaining portions of the side chains was poorer, and was not continuous in the (3Fo-2Fc) maps contoured at 1.4 $\sigma$. The remainder of the side chain of the intercalated drug was assigned 50% occupancy, but no additional density, indicating a defined alternative position, could be identified. The occupancy of the side chain of the end-stacked ligand, from carbon C18 to its terminus, was reduced to 37.5%. There was some evidence from the difference density map that this side chain interacts with the O6 as well as the N7 of guanine G6, but we were unable to fit the end of the side chain into the residual density. At the completion of refinement, the structure contains 21 water molecules with a final R factor of 21.6% and $R_{free}$ of 26.2%. The final refinement parameters are given in Table 1. Structural parameters for the DNA were analyzed using the Curves 5.2 program (Lavery and Sklenar, 1989). The coordinates and structure factors have been deposited with the Nucleic Acid Data Base, accession number DD 0023, and the Protein Data base, accession number 1DL8.

**Spectrophotometry.** Stock solutions of the 5-substituted 9-aminoacridine-4-carboxamides were prepared in ethanol and stored at 253 K. Molar extinction coefficients at the wavelength of maximum absorption in the visible spectrum were determined for the compounds free in solution, bound to calf thymus DNA, and sequestered into SDS micelles, using a Carey 219 UV/visible spectrophotometer. Measurements were made in 0.1 M SHE buffer (2 mM HEPES, 10 $\mu$M EDTA, and 99.4 mM NaCl, pH 7.0) at 293 K. Spectra were recorded at a drug concentration of 50 $\mu$M, with DNA and micelle-bound spectra determined in the presence of 1 mM calf thymus DNA (nucleotide pairs) and 10 mM SDS (monomer concentration), respectively. To determine the ability of SDS to dissociate ligand/DNA complexes, spectra of ligand/DNA mixtures were measured before and after the addition of the SDS.

**Stopped-Flow Kinetics Measurements.** Kinetic measurements were performed on a Dionex D110 stopped-flow spectrophotometer with a coupled DC amplifier, double-beam storage oscilloscope, and personal computer. The spectrophotometer was fitted with a 20-mm light path optical cuvette, giving the apparatus a dead time of about 2 ms, and was operated in transmittance mode. Data were collected and processed using software (Roos et al., 1985) that allows a wide choice of data sampling frequencies, up to every 0.1 ms. The spectrophotometer was operated with a time constant of 0.1 ms and an optical bandwidth of 3 nm. Solutions of ligand/DNA complexes containing 400 $\mu$M DNA (nucleotide pairs) and 20 $\mu$M ligand in 0.1 M SHE buffer were mixed with an equal volume of 20 mM SDS (monomer concentration) in the same buffer at 293 K. The molecular weight of the DNA was lowered by sonicating solutions containing 2 mg/ml of DNA in 0.2 M SHE buffer at 273 K for 5 min, followed by exhaustive dialysis into 0.1 M SHE buffer. Solutions were freed of particulates by passing them through 0.45-$\mu$m Millipore filters.

## Results

### Structure of the 5-F-9-Amino-DACA/d(CGTACG)$_2$ Complex

**Global Structure.** The global structure of the 5-F-9-amino-DACA/d(CGTACG)$_2$ complex is very similar to that of the isomorphous 9-amino-DACA/d(CGTACG)$_2$ complex (Adams et al., 1999). An asymmetric unit contains a single strand of DNA hexamer, one intercalated 5-F-9-amino-DACA molecule, 21 water molecules (18 of which occupy the same posi-

TABLE 1
Crystal details, data collection, and final refinement parameters

| | |
|---|---|
| Unit cell dimensions | a = 30.14 Å, c = 39.40 Å |
| Space group | $P6_4$ |
| No observations | 42095 |
| No unique reflections | 2978 |
| Resolution range (Å) | 16–1.55 |
| $R_{merge}$ (%) | 5.5 (24.3)[a] |
| Completeness (%) | 99.5 (97.3)[a] |
| I/$\sigma$I | 36.6 (4.3)[a] |
| No. of water molecules | 19 full occupancy and 2 half occupancy |
| $R_{all}$ (%) | 21.59 |
| $R_{free}$ (%) | 26.15 |
| RMSD from ideal geometry of final model distances | |
| Bonds (Å) | 0.012 (0.03)[b] |
| Angles (Å) | 0.021 (0.05)[b] |
| Planes (Å) | 0.057 (0.10)[b] |
| Average B values (Å$^2$) | |
| Bases | 16 |
| Sugars | 19 |
| Phosphates | 23 |
| Intercalated 5-F-9-amino-DACA: acridine ring | 20 |
| End-stacked 5-F-9-amino-DACA: acridine ring | 14 |
| Water | |
| Full occupancy | 26 |
| Half occupancy | 22 |

[a] Values in parentheses are for the last shell, 1.61–1.55 Å.
[b] Target values are in parentheses.

tions as in the 9-amino-DACA structure), and an additional 9-amino-DACA. No metal ions or spermine are observed in the density maps. The two strands of the DNA are related by a crystallographic dyad and form a right-handed B-DNA-like duplex with Watson-Crick base pairs. The nucleotides are labeled C1 to G6 in the 5′ to 3′ direction and the numbering scheme used for the drug is given in Fig. 1. A 5-F-9-amino-DACA molecule is intercalated between each of the CpG dinucleotide base pair steps with its side chain lying in the major groove pointing toward the center of the duplex. The partially disordered protonated terminal dimethylamino group of the carboxamide side chain refines to a position within hydrogen bonding distance of the N7 and O6 atoms of guanine G2 (Fig. 2). The additional drug molecule, on the 2-fold axis, stacks on the end of each DNA helix and links it to the next duplex to form a continuous column of duplexes in the *ab* plane with the polarity of the DNA backbone reversing at the 2-fold axis (see Fig. 2; Adams et al., 1999). The refined position of the partially disordered protonated *N*,*N*-dimethylamino group of the end-stacked ligand is in hydrogen bonding distance of the N7 atom of guanine G6. The stacked columns of duplexes lie with their helical axes in planes related by a $3_1$ axis parallel to *c*, the columns in neighboring planes intersecting in projection at the dyad axis.

**DNA Conformation.** The DNA main chain and glycosidic torsion angles, as well as the furanose conformations, are listed in Table 2. The pseudorotation angle of cytosine C1 is 358°, indicating a C2′-*exo* sugar pucker that is similar to the C3′-*endo* sugar pucker observed in the isomorphous structure (Adams et al., 1999). The *P* values for all other sugar rings fall within the normal range for the C2′-*endo* pucker of 140° to 180°. These assignments are supported by the values of the corresponding C4′-C3′ (δ) torsion angles, which are known to be correlated with sugar pucker (Neidle, 1994). The glycosidic angles, χ, are in the *medium anti* configuration range for C1 and G2, whereas for all other bases they are *high anti,* as is typically found in B-DNA (Neidle, 1994). With the exception of the phosphate P-O5′ and C5′-C4′ torsion angles α and γ at both guanine G2 and G6 residues, the main chain dihedral angles for all six nucleotides fall within ranges characteristic of B-DNA (Schneider et al., 1997). At G2 and G6, the α values have rotated by 112° and 130°, respectively, compared with those of B-DNA, and the γ values by 145° and 118°. These coupled α/γ rotations at the guanines are the principal modifications to the backbone torsion angles responsible for opening up the intercalation cavity.

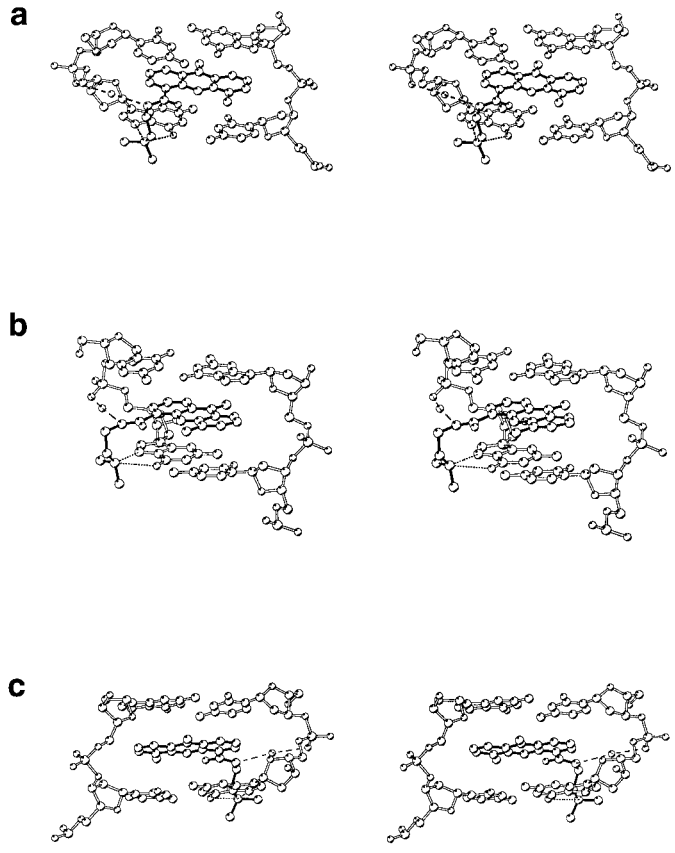


**Fig. 2.** Three stereo views of 5-F-9-amino-DACA intercalated into d(CpG) · d(GpC) and the bridging water molecule. Dashed lines indicate hydrogen bonds; dotted lines indicate distances between the O6 and N7 of guanine G2 and the refined position of the partially disordered terminal dimethylamino group. a, looking into the major groove; b, 60° rotation in *y*-axis from a; c, looking into the minor groove.

Table 3 lists the geometrical properties of the base pairs. For step 1, the rise of 6.9 Å is as expected for an intercalation cavity and its twist angle shows the DNA to be unwound by 12° at the binding site. Base pair C1-G6 has a normal B-DNA propeller twist and a positive buckle of 1.4°, whereas propeller for G2-C5 is flattened to −6° and it has a 7° buckle in the opposite direction. The roll angle is largest for step 1 and less for steps 2 and 3, but all are significantly larger than the roll angle found in canonical B-DNA. There is minimal slide, shift, and tilt at step 1. The helix winding at step 2, G2-T3, which has slide, shift, and tilt values increased slightly over step 1 but not appreciably different from B-DNA, is reduced by 8° compared with the canonical structure. In contrast to steps 1 and 2, the central T3-A4 step is overwound by 10° compared with an average B-DNA twist of 36°; however, all the other parameters are typical of B-DNA.

**Intercalated 5-F-9-Amino-DACA Conformation and DNA Interactions.** Fig. 2 shows stereo views of 5-F-9-amino-DACA intercalated via the major groove of the d(CpG) · d(GpC) binding site, which illustrates some important features of the complex. The 4-carboxamide group is planar, with the carbonyl oxygen forming an internal hydrogen bond to the protonated acridine ring nitrogen (see Table 4 for side chain dihedral angles). This interaction, coupled with a drive to maximize resonance stabilization energy between the carboxamide and the acridine chromophore, brings the carboxamide group to lie within 4° of the acridine plane. In this configuration, the carboxamide NH group points toward the sugar-phosphate backbone, where it hydrogen bonds (2.9 Å) to a water molecule that in turn hydrogen bonds (3.0 Å) to the phosphate group of guanine G2. In the refined conformation of the partially disordered portion of the side chain, the protonated *N*,*N*-dimethylaminoethyl moiety projects at right angles to the plane of the acridine ring, placing the ammonium group within hydrogen bonding distance of the N7 nitrogen (3.0 Å) and the O6 oxygen (2.9 Å) of guanine G2. The 9-amino group of the intercalated drug, which lies in the minor groove, forms no interactions with the DNA at the intercalation site, although it hydrogen bonds to the phosphate group (2.8 Å) of a symmetry-related duplex. The stacking interactions between intercalated 5-F-9-amino-DACA and the DNA bases are shown in projection in Fig. 3a.

The helix axis passes through the middle of the central acridine ring. The acridine chromophore is fully enveloped by the two base pairs and the three atoms of the 4-carboxamide group are stacked on the C4, O4, and C5 atoms of cytosine C1. Figure 3b shows the stacking pattern for the complex with 9-amino-DACA for the purposes of comparison (Adams et al., 1999).

**End-Stacked 5-F-9-Amino-DACA Conformation and DNA Interactions.** The end-stacked 5-F-9-amino-DACA molecule is sandwiched between the C1-G6 base pairs of two symmetry related hexanucleotides in the quasicontinuous stack. A second, symmetry-related, ligand molecule is superimposed on the first but flipped over along its major axis. As with the intercalated ligand, the 4-carboxamide group is planar and the carbonyl oxygen forms an internal hydrogen bond to the protonated acridine ring nitrogen (see Table 4). The carboxamide group lies within 11° of the acridine plane and the side chain projects at right angles to the plane of the chromophore in an extended conformation (Table 4). However, compared with the intercalated ligand, the refined position of the partially disordered side chain C17-C18 bond is rotated by about 90° in the direction that swings the dimethylamino group toward the DNA backbone and the C18-N19 bond is rotated about 90° in the opposite direction so as to facilitate a hydrogen bond (2.7 Å) between the protonated amine and the N7 atom of guanine G6. A water molecule forms a hydrogen-bonded bridge between the ligand 9-amino group and the phosphate group of guanine G6 in a symmetry-related duplex. There is an additional water molecule, not present in the 9-amino-DACA structure, hydrogen-bonded (2.73 Å) to the fluorine.

## Dissociation Kinetics of 5-Substituted-9-Amino-DACA/Calf Thymus DNA Complexes

In Table 5, we present the visible absorption spectra of the series of 5-substituted 9-amino-DACA derivatives studied, free in aqueous solution, bound to calf thymus DNA, and sequestered into SDS micelles. As expected, the compounds show absorption maxima around 410–440 nm, with molar extinction coefficients of about $10^4$ (Wakelin et al., 1987). When complexed with DNA, the spectra of all the ligands exhibit the bathochromic shifts and large hypsochromic effect, the latter of about 40 to 60%, characteristic of intercalative binding. Despite steric effects on protonation that lower chromophore p$K_a$ values slightly, even for compounds with electron-donating substituents (Denny et al., 1987), all

TABLE 2
Sugar-phosphate torsion angles, glycosidic angles (degrees), and furanose conformations for 5-F-9-amino-DACA[a]

| | $\alpha$ P-O5′ | $\beta$ O5′-C5′ | $\gamma$ C5′-C4′ | $\delta$ C4′-C3′ | $\varepsilon$ C3′-O3′ | $\zeta$ O3′-P | $\chi$ C1′-N | $P$ | $\tau_m$ | Pucker |
|---|---|---|---|---|---|---|---|---|---|---|
| C1 | | | 62 | 86 | −163 | −74 | −137 | 358 | 44 | C2′-*exo* |
| G2 | −174 | 174 | −167 | 158 | −175 | −108 | −115 | 178 | 41 | C2′-*endo* |
| T3 | −67 | −177 | 49 | 146 | −133 | −179 | −90 | 152 | 41 | C2′-*endo* |
| A4 | −66 | 151 | 56 | 142 | 177 | −99 | −100 | 158 | 33 | C2′-*endo* |
| C5 | −69 | 174 | 55 | 141 | −150 | −161 | −94 | 142 | 45 | C2′-*endo* |
| G6 | 68 | 161 | −70 | 165 | | | −72 | 174 | 38 | C2′-*endo* |
| B-DNA[b] | −62 | $B_I$ 176<br>$B_{II}$ 146 | 48 | $B_I$ 128<br>$B_{II}$ 144 | $B_I$ −176<br>$B_{II}$ −114 | $B_I$ −95<br>$B_{II}$ 174 | $B_I$ −102<br>$B_I$Y −119<br>$B_{II}$ −89 | 160 | 35 | C2′-*endo* |

$P$, the pseudorotation phase angle; $\tau_m$, the pseudorotation amplitude.
[a] All parameters were calculated using the Curves 5.2 program (Lavery and Sklenar, 1989).
[b] Average values for B DNA taken from Schneider et al. (1997).

TABLE 3
Geometrical properties of base-pair steps and base pairs for 5-F-9-amino-DACA[a]

| Base Pair | Step | Shift | Slide | Rise | Tilt | Roll | Twist | Propeller Twist | Buckle |
|---|---|---|---|---|---|---|---|---|---|
| | | *Å* | *Å* | *Å* | *deg* | *deg* | *deg* | *deg* | *deg* |
| C1-G6 | | | | | | | | −10 | 1.4 |
| | 1 | 0.1 | 0.1 | 6.9 | 0.1 | 4.9 | 24 | | |
| G2-C5 | | | | | | | | −6 | −7.0 |
| | 2 | −0.3 | −0.6 | 3.3 | −0.6 | 3.1 | 28 | | |
| T3-A4 | | | | | | | | −10 | 1.1 |
| | 3 | 0.0 | 0.6 | 3.2 | 0.0 | −2.9 | 46 | | |
| A4-T3 | | | | | | | | −10 | −1.0 |
| B-DNA[b] | | 0 | 0 | 3.4 | 2 | 1 | 36 | −11 | |

deg, degrees.
[a] All parameters were calculated using the Curves 5.2 program (Lavery and Sklenar, 1989).
[b] Average values for B DNA taken from Neidle (1994).

TABLE 4
Refined 5-F-9-Amino-DACA side chain torsion angles (degrees)

| | 5-F-9-amino-DACA Torsion Angle[a] | | | | | |
|---|---|---|---|---|---|---|
| | 1 | 2 | 3 | 4 | 5 | 6 |
| Intercalated[b] | 4 (5) | −177 (4) | −79 (10) | −37 (10) | 171 (9) | −65 (10) |
| End-stacked[b] | −11 (7) | 171 (7) | 102 (9) | 46 (9) | 81 (8) | −153 (5) |

[a] Torsion angle definition: 1 = C3 - C4 - C15 - N16; 2 = C3 - C4 - C15 - O15; 3 = C15 - N16 - C17 - C18; 4 = N16 - C17 - C18 - N19; 5 = C17 - C18 - N19 - C20; 6 = C17 - C18 - N19 - C21.
[b] Torsion angles 3 to 6 are given for the refined position of the partially disordered terminal dimethylamino group.

of the compounds have chromophore p$K_a$ values sufficiently high that they are likely to be dicationic when bound to DNA at pH 7 (see Table 7). This is probable even for compound **7**, the $SO_2Me$ derivative, because p$K_a$ values are known to rise on intercalation (see Jones and Wilson, 1981; Misra and Honig, 1995). That the compounds studied do indeed have high DNA binding constants typical of dications is shown by their affinities for the alternating DNA copolymers given in Table 7. On sequestering into SDS micelles, ligand absorption maxima generally move to slightly longer wavelengths, but there is little effect on molar extinction coefficients (Table 5). Adding SDS to preformed ligand/DNA complexes fully dissociates the complexes as evidenced by the reversion of absorption spectra to those of the free ligand in SDS solution (data not shown).

Kinetic measurements were made at, or close to, the wavelength of maximum absorption of the ligand in SDS, where the differential absorbance between DNA-bound versus micelle-bound ligand is greatest. No time-resolvable changes were seen when solutions of free ligand and detergent were mixed in the stopped-flow instrument, indicating that the changes observed in the presence of DNA can be solely attributed to dissociation of the ligand/DNA complexes. The multiple first-order dissociation curves were deconvoluted into their exponential components as described previously (Roos et al., 1985). Data from at least six kinetic runs were analyzed separately and the results were averaged. Table 6 gives the resolved time constants $\tau$ and their associated amplitudes, A. In all cases, the absolute values of the amplitudes sum to the equilibrium absorbance change, indicating that all of the dissociation processes are within the time range of the instrument. The arithmetic mean time constants and mean dissociation rates are also included, as single kinetic measures to aid in intercompound comparisons and to assist in formulating correlations between kinetics, thermodynamics, and biological activity. Given that the ligand-to-DNA binding ratio is one drug molecule per two turns of the helix, that 9-amino-DACA binds selectively to GC-rich DNA as a consequence of side chain-guanine interactions (Bailly et al., 1992; Adams et al., 1999), and that the dissociation kinetics for binding of 9-amino-DACA to poly[d(G-C)] and calf thymus DNA are indistinguishable at this binding ratio (Wakelin et al., 1987), it seems probable that, for the compounds studied, the kinetic measurements are reporting dissociation parameters for high-affinity GC-rich binding sites. That the 5-substituted series do in general share a preference for binding to GC-rich DNA is shown in Table 7, and the crystallographic results presented here confirm the capacity of their 4-carboxamide side chains to maintain the specific hydrogen bonding interaction with guanine, at least for the 5-F derivative.

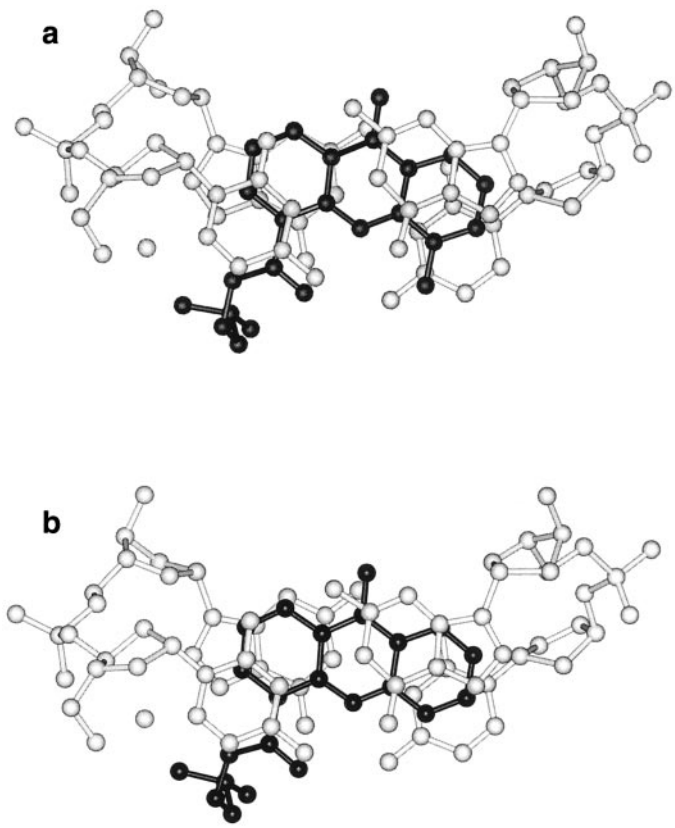


**Fig. 3.** Projection down the helix axis of a d(CpG) · d(GpC) dinucleotide with sandwiched intercalated ligand (drawn in black). a, 5-F-9-amino-DACA complex; b, 9-amino-DACA complex.

With the exception of the *p*-aminophenyl derivative, compound **14**, Table 6 shows that the patterns of dissociation for the 5-substituted ligands are qualitatively similar to that of 9-amino-DACA, inasmuch as the dissociation profiles deconvolute into four resolvable components. This is strong evidence that, except for compound **14**, the mechanism of dissociation is constant across the series and is the same as found for the parent compound. For the ligands bearing nonphenyl 5-substituents, compounds **2** to **11**, all individual dissociation time constants are larger than those of 9-amino-DACA, regardless of the steric, hydrophobic, H-bonding, or electronic properties of the substituents. On average, compared with the parent, $\tau_1$ is slowed 2.1-fold, $\tau_2$ by 3.0-fold, $\tau_3$ by 4.2-fold, and $\tau_4$ by 3.7-fold. Generally speaking, 5-substitution enhances the proportion of the dissociation reaction represented by A2 at the expense of the other three components. The outcome of these individual changes is that, across the series, the average mean dissociation rate falls 3-fold from 8.6 $s^{-1}$ for 9-amino-DACA to 2.9 $s^{-1}$. In a similar vein, the tetracyclic 5,6-benz derivative, compound **15,** which may be regarded as a 5,6-bis-substituted derivative, seems to dissociate by the same mechanism as 9-amino-DACA, only much more slowly still, with a mean dissociation rate about 14-fold less.

The 5-phenyl analogs, compounds **12**, **13**, and **14**, behave somewhat differently from their nonaromatic homologs. The unsubstituted 5-phenyl derivative, **12**, dissociates about twice as fast as 9-amino-DACA, with each component time constant approximately doubling. Adding a *p*-nitro group to the phenyl ring, compound **13**, returns the kinetic profile to one that is almost indistinguishable from 9-amino-DACA, giving a mean dissociation rate of 8.3 $s^{-1}$. The dissociation profile for the *p*-aminophenyl derivative, compound **14**, comprises five exponential components, all of which are substantially slower than those found for 9-amino-DACA. The fifth component has the remarkably long time constant of 29 s and the four faster exponentials are slowed 3.6- to 11-fold. Clearly, compound **14** dissociates by a mechanism different from that of the other ligands studied and has a mean dissociation rate 15-fold slower than 9-amino-DACA.

## Discussion

The acridine-4-carboxamides are now well established as a class of DNA intercalating agent that poisons topoisomerases I and II and that yields cytotoxic compounds with in vivo activity against both experimental leukemias and solid tumors (Atwell et al., 1984, 1987; Denny et al., 1986, 1987; Rewcastle et al., 1986; Schneider et al., 1988; Baguley et al., 1995; Finlay et al., 1996). Denny and colleagues have suggested that solid tumor activity may be correlated with the capacity to inhibit both topoisomerases simultaneously and with the possession of an uncharged chromophore to promote tissue distribution (Denny et al., 1987; Denny, 1997). Our kinetic and structural studies of the interaction of 9-aminoacridine-4-carboxamides with DNA and oligonucleotides have helped define some of the molecular determinants involved in selectively poisoning topoisomerase II (Wakelin et al., 1987; Adams et al., 1999; Todd et al., 1999; and see the Introduction): an activity associated with possession of an acridine 9-amino substituent and with in vivo activity confined to disseminated tumors (Atwell et al., 1984; Rewcastle

TABLE 5
Spectroscopic properties of 5-substituted 9-aminoacridinecarboxamides

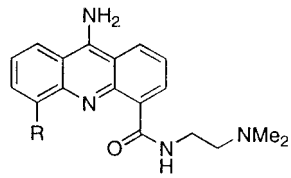


| No. | R | Free | | DNA-Bound | | SDS-Bound | | $\Delta\varepsilon^c$ |
|---|---|---|---|---|---|---|---|---|
| | | $\lambda^a$ | $\varepsilon^b$ | $\lambda$ | $\varepsilon$ | $\lambda_{max}$ | $\varepsilon$ | |
| **1** | H | 407 | 9.4 | 421 | 4.9 | 415 | 9.4 | 4.5 |
| **2** | F | 410 | 12 | 423 | 5.5 | 423 | 12 | 7.8 |
| **3** | Cl | 434 | 11 | 448 | 5.9 | 439 | 12 | 6.6 |
| **4** | Br | 435 | 8.5 | 449 | 4.4 | 439 | 9.3 | 5.3 |
| **5** | $CF_3$ | 429 | 11 | 439 | 6.0 | 432 | 13 | 7.8 |
| **6** | $NO_2$ | 447 | 9.6 | 459 | 5.1 | 450 | 12 | 7.3 |
| **7** | $SO_2CH_3$ | 439 | 9.9 | 447 | 5.7 | 435 | 10 | 5.5 |
| **8** | $NH_2$ | 435 | 6.9 | 453 | 5.7 | 444 | 5.8 | 2.8 |
| **9** | $CH_3$ | 413 | 9.1 | 427 | 4.9 | 416 | 9.8 | 5.4 |
| **10** | $OCH_3$ | 421 | 8.6 | 437 | 4.6 | 424 | 8.9 | 4.8 |
| **11** | OPr | 421 | 10 | 438 | 5.3 | 424 | 11 | 6.2 |
| **12** | Ph | 416 | 10 | 430 | 4.9 | 419 | 11 | 5.5 |
| **13** | Ph-*p*-$NO_2$ | 415 | 15 | 428 | 8.1 | 418 | 15 | 8.4 |
| **14** | Ph-*p*-$NH_2$ | 421 | 11 | 441 | 6.5 | 441 | 11 | 4.5 |
| **15** | 5,6-Benz | 407 | 6.5 | 420 | 4.1 | 407 | 7.7 | 4.6 |

Ph, phenyl; OPr, propoxy.
[a] Absorbance maximum, nm.
[b] Molar extinction coefficient $\times 10^{-3}$.
[c] Difference in molar extinction coefficient between SDS-bound and DNA-bound ligand at the wavelength used in the kinetic studies.

TABLE 6
Dissociation time constants of 5-substituted 9-aminoacridinecarboxamides

| No. | R | Time Constants | | | | Amplitudes | | | | $\tau^a$ | $\tau^{-1b}$ |
|---|---|---|---|---|---|---|---|---|---|---|---|
| | | $\tau_1$ | $\tau_2$ | $\tau_3$ | $\tau_4$ | A1 | A2 | A3 | A4 | | |
| | | *ms* | | | | % | | | | *s* | $s^{-1}$ |
| **1** | H | 6 | 28 | 86 | 428 | 14 | 34 | 34 | 18 | 0.12 | 8.6 |
| **2** | F | 6 | 66 | 480 | 1900 | 13 | 58 | 15 | 15 | 0.40 | 2.5 |
| **3** | Cl | 8 | 93 | 410 | 2400 | 12 | 48 | 28 | 12 | 0.45 | 2.2 |
| **4** | Br | 10 | 91 | 360 | 2200 | 10 | 46 | 31 | 13 | 0.44 | 2.3 |
| **5** | $CF_3$ | 12 | 61 | 210 | 1300 | 8 | 58 | 28 | 7 | 0.18 | 5.4 |
| **6** | $NO_2$ | 9 | 67 | 430 | 1600 | 8 | 56 | 25 | 10 | 0.30 | 3.3 |
| **7** | $SO_2CH_3$ | 13 | 78 | 300 | 1100 | 4 | 41 | 31 | 24 | 0.39 | 2.6 |
| **8** | $NH_2$ | 21 | 120 | 500 | 1700 | 17 | 52 | 23 | 8 | 0.32 | 3.2 |
| **9** | $CH_3$ | 21 | 110 | 320 | 1400 | 10 | 43 | 30 | 17 | 0.38 | 2.6 |
| **10** | $OCH_3$ | 17 | 69 | 300 | 1100 | 4 | 20 | 53 | 23 | 0.43 | 2.3 |
| **11** | OPr | 9 | 78 | 310 | 1100 | 8 | 29 | 50 | 13 | 0.32 | 3.1 |
| **12** | Ph | 4 | 11 | 39 | 200 | 5 | 33 | 45 | 17 | 0.056 | 18 |
| **13** | Ph-*p*-$NO_2$ | 7 | 25 | 84 | 460 | 10 | 32 | 40 | 17 | 0.12 | 8.3 |
| **14**[c] | Ph-*p*-$NH_2$ | 23 | 100 | 600 | 4600 | 59 | 26 | 4 | 6 | 1.8 | 0.56 |
| **15** | 5,6-Benz | 36 | 400 | 1600 | 6200 | 8 | 37 | 41 | 14 | 1.7 | 0.60 |

Ph, phenyl; OPr, propoxy.
[a] $\tau$, average dissociation time constant, s ($\tau = \Sigma_r A_r \tau_r$).
[b] $\tau^{-1}$, average dissociation rate constant, $s^{-1}$ ($\tau^{-1} = 1/\tau$).
[c] Fifth transient observed ($\tau_5$ = 29,000 ms; A5 = 5%).

et al., 1986). Importantly, substituting 9-amino-DACA in the 5 position enhances cytotoxic potency and, with strongly electron withdrawing substituents, widens the in vivo tumor spectrum to include solid tumors (Denny et al., 1987). These are properties that have obvious relevance to the potential clinical development of the 9-aminoacridine-4-carboxamides. In this work, we present our first description of the refined structure of a 5-substituted 9-amino-DACA derivative bound to a DNA hexanucleotide and a kinetic characterization of the interaction of a series of such ligands bound to mammalian DNA.

A major finding is that 5-F-9-amino-DACA binds to $d(CGTACG)_2$ in a manner similar to that of the parent compound, indicating that variations in the biological properties of 5-substituted 9-amino-DACAs are not likely to be associated with gross re-arrangement of the structure of the DNA-ligand complex. Among the most significant features that the two complexes have in common is intercalation at the CpG dinucleotide step, the possession of an internally hydrogen-bonded planar carboxamide group, which in turn is hydrogen bonded via a bridging water molecule to a phosphate oxygen at the intercalation site, and hydrogen bonding interactions between the protonated *N*,*N*-dimethylammonium group of the ligand side chain and the O6 and N7 atoms of guanine. The DNA main chain torsion angles and sugar puckers are effectively indistinguishable in the two complexes as is the pattern and distribution of fixed water molecules. The major differences in DNA structure center on the perturbation of base pair winding angles consequent on intercalation. Binding by 5-F-9-amino-DACA unwinds the CpG and GpT steps by 12° and 8°, respectively, and overwinds the TpA step by 10° compared with the canonical B-DNA value of 36°. The corresponding values for 9-amino-DACA are 8°, 12°, and 17° (Adams et al., 1999). Thus, the total unwinding of the first two steps is the same for the two complexes, but the overwinding of the central TpA base pairs is substantially less in the case of the 5-F derivative. The overall DNA conformation for the 5-F-9-amino-DACA complex is more similar to canonical B-DNA than is that of the 9-amino-DACA complex. A notable feature of the 5-F-9-amino-DACA complex is the stacking of the 5-F atom on the C4 atom of cytosine C5 at the CpG intercalation site. Significantly, it appears that the position of the cytosine ring has moved, relative to guanine G6, within the helical stack to maximize this interaction (see Fig. 3, a and b).

The most important findings from the kinetics studies are that, with the exception of the *p*-aminophenyl derivative, the mechanism of binding seems constant across the series and, putting aside the 5-phenyl compounds in general, dissociation rates are slowed for all derivatives regardless of their size, hydrophobicity, and electronic properties [see Table 7, where the compounds are arranged in descending order of $\tau_4$, the kinetic parameter that segregates with cytotoxicity for a series of 5-H 9-aminoacridinecarboxamides (Wakelin et al., 1987)]. Thus, as implied from our crystallographic results, which show that complexes of the 5-H and 5-F derivatives have essentially the same structure, there is no evidence from the kinetic studies of a change in binding mechanism for the 5-substituted derivatives that could account for their enhanced biological properties. Taking the crystal structures of the DNA complexes of 9-amino-DACA and the 5-F derivative as typical of the series as a whole, then it seems that the major factor contributing to the greater kinetic stability of complexes of 5-substituted ligands is increased stacking interactions with cytosine in the preferred CpG binding site. If so, dissociation rates would be expected to be minimized for the 5,6-benz derivative where intermolecular $\pi$-orbital interactions would be maximized, as is found experimentally (Table 6). Variations in the energetics of overwinding adjacent AT-rich sequences may also contribute to stabilizing the complex.

Multiple linear regression analysis using Pearson product-moment correlation methods failed to reveal any statistically significant correlations between dissociation rates and molecular descriptors ($\sigma$ and $\pi$ electronic factors, molecular refractive index, $pK_a$, and an indicator for hydrogen bonding

TABLE 7
Equilibrium, kinetic, and biological properties of 5-substituted 9-aminoacridinecarboxamides

| No. | R | $pK_a$[a] | log*K*[b] | | $IC_{50}$ L1210[c] | ILS %[d] | Kinetics | |
|---|---|---|---|---|---|---|---|---|
| | | | (AT) | (GC) | | P388 | $\tau^{-1}$ | $\tau 4$ |
| | | | | | *nM* | | $s^{-1}$ | *s* |
| **14** | Ph-*p*-$NH_2$ | 7.5[e] | 7.46 | 7.64 | 5.5 | 68 | 0.56 | 29[f] |
| **15** | 5,6-Benz | | | | | | 0.60 | 6.2 |
| **3** | Cl | 6.87 | 7.48 | 7.23 | 2.9 | 81 | 2.2 | 2.4 |
| **4** | Br | 6.56 | 7.93 | 8.00 | 2.5 | 82 | 2.3 | 2.2 |
| **2** | F | 7.11 | 7.90 | 8.18 | 1.4 | 90 | 2.5 | 1.9 |
| **8** | $NH_2$ | 7.41 | 8.14 | 8.10 | 18 | 32 | 3.2 | 1.7 |
| **6** | $NO_2$ | 6.59 | 8.41 | 8.41 | 1.6 | 39 | 3.3 | 1.6 |
| **9** | $CH_3$ | 8.01 | 7.55 | 7.86 | 0.47 | 107 | 2.6 | 1.4 |
| **5** | $CF_3$ | 5.89 | 7.85 | 8.03 | 5.7 | 115 | 5.4 | 1.3 |
| **10** | $OCH_3$ | 7.80 | 7.62 | 7.83 | 4.3 | 81 | 2.3 | 1.1 |
| **7** | $SO_2CH_3$ | 5.15 | 7.32 | 8.30 | 2.8 | 138 | 2.6 | 1.1 |
| **11** | OPr | 7.82 | 8.00 | 7.92 | 3.3 | 47 | 3.1 | 1.1 |
| **13** | Ph-*p*-$NO_2$ | 7.5[e] | 7.05 | 7.35 | 3.6 | 65 | 8.3 | 0.46 |
| **1** | H | 8.30 | 7.08 | 7.55 | 15 | 98 | 8.6 | 0.43 |
| **12** | Ph | 7.50 | 6.92 | 7.41 | 1.1 | 54 | 18 | 0.2 |

Ph, phenyl; OP, propoxy.
[a] Values from Denny et al. (1987).
[b] logK, binding constant to poly[d(A-T)] or poly[d(G-C)], determined by ethidium bromide displacement; from Denny et al. (1987).
[c] Concentration required to inhibit growth of L1210 cells by 50%, from Denny et al. (1987).
[d] Increase in life span of mice bearing P388 and Lewis lung tumors, from Denny et al. (1987).
[e] Estimated.
[f] Slowest observed transient, $\tau_5$.

potential) for the compound set, which excluded the substituted phenyl and 5,6-benz derivatives. This may be a consequence of the limited range of the dependent variables. However, inspecting Table 7 shows that there is an apparent relationship between $\tau_4$ and the nature of the 5-substituent for these compounds, which can be rationalized in general terms. The first 5 in rank order (**3**, **4**, **2**, **8**, and **6**) have $\tau_4$ values ranging from 2.4 to 1.6 s, and in this subset, R is small and the atom directly connected to the acridine C5 position has occupied *p* or *d* orbitals. These five substituents have the capacity to stack neatly on cytosine within the DNA duplex and the correct frontier orbital symmetry to interact favorably via a charge-transfer mechanism with the $\pi$-orbitals of the GC-base pairs. The next two compounds in the rank order, **9** and **5**, are the hydrophobic methyl and trifluoromethyl derivatives with $\tau_4$ values of 1.4 and 1.3 s. These R groups would also fit snugly within the base pair stack, stabilizing the complex by both van der Waals interaction with the cytosine and by hydrophobic effects as a consequence of their complete removal from solvent. Compounds **10**, **7**, and **11**, the methylsulfone, methoxy, and propoxy derivatives, cluster at $\tau_4$ = 1.1 s. These substituent groups are bulkier and more water soluble and, in the DNA complex, would protrude into the solvent, which may weaken their van der Waals and hydrophobic contributions to the stacking energy. The remaining compounds in the list are the parent 9-amino-DACA and the phenyl derivative, which is discussed separately below.

The kinetic findings for the 5-phenyl compounds stand apart from those of the nonaromatic derivatives and are more difficult to understand. The kinetic profiles for the unsubstituted derivative, compound **12,** and its *p*-nitro derivative, compound **13**, conform to that of 9-amino-DACA, implying the binding mechanism is the same. Inspection of the crystal structures makes it clear that the 5-phenyl ring would collide unfavorably with cytosine in the binding site, leading to increased dissociation rates and lower affinities, as is found experimentally for compound **12** (Tables 6 and 7). Curiously, the addition of a *p*-nitro substituent reinstates the kinetic and thermodynamic parameters to those typical of 9-amino-DACA. The reasons for this are unclear but may be related to substituent-induced changes in acridine-phenyl rotamer conformation, so as to bring the phenyl ring more into the plane of the intercalation cavity. Alternatively, they may be related to the issue that the increased surface area of the *p*-nitrophenyl ring provides a greater impediment to dissociation as a result of the necessity to displace more solvent molecules on exit (see Wakelin and Waring, 1980). The *p*-aminophenyl derivative, compound **14**, has extraordinarily slow dissociation kinetics and has acquired an additional step in its dissociation pathway. Evidently it binds by a similar but different and unknown mechanism. Molecular models suggest the *p*-aminophenyl group may form additional hydrogen bonding interactions with a phosphate group at the intercalation site.

The multiple linear regression analysis described above also failed to reveal any statistically significant correlations between affinity, dissociation rates, cytotoxic potency, and the chosen molecular descriptors. Again, this seemed to be a consequence of the limited range of the dependent variables. However, across the series as a whole, the average dissociation rate is 3-fold lower compared with that of 9-amino-DACA, which compares with a 3-fold increase in average binding affinity to poly[d(G-C)] (see Table 7). Thus, there is the expected broad relationship between affinity and dissociation kinetics, with the observed 10-fold range in affinity being matched by an 8-fold variation in $\tau^{-1}$ and a 12-fold variation in $\tau_4$. Deviations from a strict correlation between affinity and dissociation rate (i.e., lack of adherence to a perfect linear free energy relationship) for individual compounds is presumably related to minor variations in the kinetics of association, which are too fast to measure by stopped-flow methods. Notwithstanding the lack of a statistically significant correlation between ligand structure and cytotoxicity, if the compounds are ranked according to their cytotoxic potency, it is possible to discern potential relationships between activity and the nature of the 5-substituent. First, with the exception of the 5-amino derivative, all the compounds studied are more cytotoxic than the parent compound. On average, a 5-substituted derivative is 4-fold more potent than 9-amino-DACA, a degree of enhancement that compares with the average 3-fold increase in affinity and 3-fold slowing in dissociation rate for the series. This finding suggests a general class relationship between activity, affinity, and kinetics in which stabilizing the complex enhances activity. That the 5-amino derivative is less active but thermodynamically and kinetically more stable than 9-amino-DACA hints at the possibility that the hydrogen bond-donating amino group also interacts, unfavorably, with topoisomerase II in the ternary complex. If so, this may imply that the protein itself offers a hydrogen bond donor at this location, an idea that could account for the rank order of potency of the nitro, methylsulfone, propoxy, methoxy, and trifluoromethyl derivatives. The notion that the 5-substituent might also interact directly with the topoisomerase protein is strengthened by the finding that the phenyl and *p*-nitrophenol derivatives are more cytotoxic than 9-amino-DACA despite having faster dissociation kinetics and lower binding affinities. In this case, however, the phenyl ring seems to interact favorably with the topoisomerase.

Taken as a whole, our kinetic, sequence preference and crystallographic studies (Wakelin et al., 1987; Bailly et al., 1992; Adams et al., 1999; Todd et al., 1999; this work) strongly suggest that the 9-aminoacridine-4-carboxamides inhibit topoisomerase II by intercalating into CpG dinucleotide sequences with their protonated *N*,*N*-dimethylaminoethyl side chains making hydrogen bonding interactions to the O6 and N7 atoms of guanine in the major groove. As described previously (Adams et al., 1999), we believe that the 4-carboxamide side chain, in addition to depriving the enzyme access to these hydrogen bonding groups of guanine, also makes direct interaction with the protein. Considering all the findings presented here, we conclude that substituents in the acridine 5 position, which strongly modify biological activity, do so either by kinetically stabilizing the DNA complex by favorable stacking interactions with cytosine in the intercalation cavity, or by interacting directly with topoisomerase II. We note that this description of the mode of action of the acridine-4-carboxamides places their active side chains in the major groove of DNA, which is the groove opposite the location of the side chain of the anthracyclines doxorubicin and daunomycin (Frederick et al., 1990). This necessarily means that the two drug classes inhibit topoisomerase II by radically different mechanisms, which suggests that should tumors become resistant to anthracycline ther-

apy as a consequence of mutations to the enzyme, they might not be cross-resistant to acridine-4-carboxamide treatment. Last, we note that because stacking interactions with cytosine in CpG sequences seem to be an important determinant of biological activity for the acridine-4-carboxamides, and that van der Waals interactions would probably be enhanced between 5-substituted 9-amino-DACAs and 5-methylcytosines, it is conceivable that 5-methylcytosine found in the CpG islands involved in the transcriptional control sequences of many genes (Toyota and Issa, 1999) may provide a "hot spot" for binding 5-substituted 9-aminoacridine-4-carboxamides in vivo. If so, the location of topoisomerase II-induced lesions at these strategic sites may contribute to their enhanced cytotoxicity and wider tumor spectrum.

**References**


Adams A, Guss JM, Collyer CA, Denny WA and Wakelin LPG (1999) Crystal structure of the topoisomerase poison 9-amino-[N-(2-dimethylamino)ethyl]acridine bound to the DNA hexanucleotide d(CGTACG)$_2$. *Biochemistry* **38:**9221–9233.

Atwell GJ, Cain BF, Baguley BC, Finlay GJ and Denny WA (1984) Potential antitumor agents 43. Synthesis and biological activity of dibasic 9-aminoacridine-4-carboxamides, a new class of antitumor agent. *J Med Chem* **27:**1481–1485.

Atwell GJ, Rewcastle GW, Baguley BC and Denny WA (1987) Potential antitumor agents. 50. In vivo solid tumor activity of derivatives of (N-[2-(dimethylamino)ethyl]acridine-4-carboxamide). *J Med Chem* **30:**664–669.

Baguley BC, Zhuang L and Marshall EM (1995) Experimental solid tumor activity of (N-[2-(dimethylamino)ethyl]acridine-4-carboxamide). *Cancer Chemother Pharmacol* **36:**244–248.

Bailly C, Denny WA, Mellor LE, Wakelin LPG and Waring MJ (1992) Sequence specificity of the binding of antitumor amsacrine-4-carboxamides to DNA studied by DNase I footprinting. *Biochemistry* **31:**3514–3524.

Crenshaw JM, Graves DE and Denny WA (1995) Interactions of acridine antitumor agents with DNA: Binding energies and groove preferences. *Biochemistry* **34:** 13682–13687.

Denny WA (1997) Dual topoisomerase I/II poisons as anticancer drugs. *Exp Opin Invest Drugs* **6:**1845–1851.

Denny WA, Roos IAG and Wakelin LPG (1986) Inter-relationships between antitumor activity, DNA breakage and DNA binding kinetics for 9-aminoacridine-4-carboxamide antitumor agents. *Anti-Cancer Drug Design* **1:**141–147.

Denny WA, Atwell GJ, Rewcastle GW and Baguley BC (1987) Potential antitumor agents. 49. 5-Substituted derivatives of N-[2-(dimethylamino)ethyl]-9-aminoacridine-4-carboxamide with in vivo solid tumor activity. *J Med Chem* **30:**658–663.

Finlay GJ, Riou J-F and Baguley BC (1996) From amsacrine to DACA (N-[2-(dimethylamino)ethyl]acridine-4-carboxamide): Selectivity for topoisomerases I and II among acridine derivatives. *Eur J Cancer* **32:**708–714.

Frederick CA, Williams LD, Ughetto G, van der Marel GA, van Boom JH, Rich A and Wang AH-J (1990) Structural comparison of anticancer drug-DNA complexes: Adriamycin and daunomycin. *Biochemistry* **29:**2538–2549.

Insight II User Guide (1995) Biosym/MSI, San Diego, CA.

Jones RL and Wilson WD (1981) Effects of ionic strength on the pKa of ligands bound to DNA. *Biopolymers* **20:**141–154.

Jones TA, Zou JY, Cowan SW and Kjeldgaard M (1991) Improved methods for building protein models in electron density maps and the location of errors in these models. *Acta Crystallogr A* **47:**110–119.

Kestell P, Dunlop I, McCrystal MR, Evans BD, Paxton JW, Gamage RS and Baguley BC (1999) Plasma pharmacokinetics of N-[2-(dimethylamino)ethyl]acridine-4-carboxamide in phase I trial. *Cancer Chemother Pharmacol* **44:**45–50.

Lavery R and Sklenar H (1989) Defining the structure of irregular nucleic acids: Conventions and principles. *J Biomol Struct Dyn* **6:**655–667.

Malonne H and Atassi G (1997) DNA topoisomerase targeting drugs: Mechanisms of action and perspectives. *Anti-Cancer Drugs* **8:**811–822.

McCrystal MR, Evans BD, Harvey VJ, Thompson PI, Porter DJ and Baguley BC (1999) Phase I study of the cytotoxic agent N-[2-(dimethylamino)ethyl]acridine-4-carboxamide. *Cancer Chemother Pharmacol* **44:**39–44.

Misra VK and Honig B (1995) On the magnitude of the electrostatic contribution to ligand-DNA interactions. *Proc Natl Acad Sci USA* **92:**4691–4695.

Neidle S (1994) *DNA Structure and Recognition* (Rickwood D ed), IRL Press at Oxford University Press, Oxford, UK

Otwinowski Z (1993) Oscillation data reduction program, in *Proceedings of the CCP4 Study Weekend: Data Collection and Processing* (Sawyer L, Isaacs N and Bailey SS eds) pp 56–62, SERC, Daresbury Laboratory, Warrington, UK.

Palmer BD, Rewcastle GW, Atwell GJ, Baguley BC and Denny WA (1988) Potential antitumor agents 54. Chromophore requirements for *in vivo* antitumor activity among the general class of linear tricyclic carboxamides. *J Med Chem* **31:**707–712.

Rewcastle GW, Atwell GJ, Chambers D, Baguley BC and Denny WA (1986) Potential antitumor agents. 46. Structure-activity relationships for acridine monosubstituted derivatives of the antitumor agent N-[2-(dimethylamino)ethyl]-9-aminoacridine-4-carboxamide. *J Med Chem* **29:**472–477.

Roos IAG, Wakelin LPG, Hakkennes J and Coles J (1985) Collection and analysis of kinetic data from a stopped-flow spectrophotometer using a microcomputer. *Anal Biochem* **146:**287–298.

Schneider E, Darkin SA, Lawson PA, Ching L-M, Ralph RK and Baguley BC (1988) Cell line selectivity and DNA breakage properties of the antitumor agent (N-[2-(dimethylamino)ethyl]acridine-4-carboxamide): Role of topoisomerase II. *Eur J Cancer Clin Oncol* **24:**1783–1790.

Schneider B, Neidle S and Berman HM (1997) Conformations of the sugar-phosphate backbone in helical DNA crystal structures. *Biopolymers* **42:**113–124.

Sheldrick GM (1997) *The SHELX-97 Manual*. University of Göttingen, Göttingen, Germany.

Taylor R and Kennard O (1982) Molecular structures of nucleosides and nucleotides. 2. Orthogonal coordinates for standard nucleic acid base residues. *J Am Chem Soc* **104:**3206–3212.

Todd AK, Adams A, Thorpe JH, Denny WA, Wakelin LPG and Cardin CJ (1999) Major Groove binding and a 'DNA-induced' fit in the intercalation of a derivative of the mixed topoisomerase I/II inhibitor (N-(2-dimethylamino)ethyl)acridine-4-carboxamide (DACA) into DNA; X-ray structure complexed to d(CG(5-Br)ACG)$_2$ at 1.3 Å resolution. *J Med Chem* **42:**536–540.

Toyota M and Issa JP (1999) CpG island methylator phenotypes in ageing and cancer. *Semin Cancer Biol* **9:**349–357.

Wakelin LPG, Atwell GJ, Rewcastle GW and Denny WA (1987) Relationships between DNA binding kinetics and biological activity for the 9-aminoacridine-4-carboxamide class of antitumor agents. *J Med Chem* **30:**855–862.

Wakelin LPG and Waring M (1980) Kinetics of drug-DNA interaction: Dependence of the binding mechanism on structure of the ligand. *J Mol Biol* **144:**183–214.


**Send reprint requests to:** Dr. Adrienne Adams, Department of Biochemistry, University of Sydney, NSW 2006, Australia. E-mail: a.adams@biochem.usyd.edu.au